Analytical Methods

Accepted Manuscript

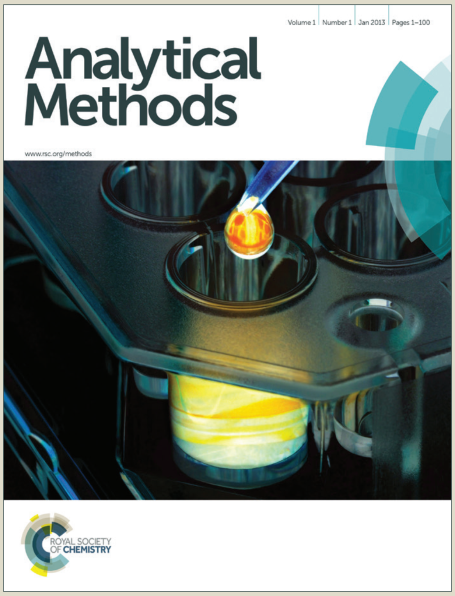

ROYAL SOCIETY
OF CHEMISTRY

www.rsc.org/methods

THE RESEARCH OF TEMPERATURE PROPERTIES OF PHOTOACOUSTIC SPECTROSCOPY DETECTION FOR SF_6 DECOMPOSITION PRODUCTS IN GAS INSULATED SWITCHGEAR

J. Luo[a], Y. H. Fang[a]*, Z. X. Su[b], D. C. Li[a], ,Y. D. Zhao[a], A. J. Wang[a], J. Wu[a], F. X. Cui[a], Y. Y. Li[a]

[a] *Key Laboratory of Optical Calibration and Characterization, Anhui Institute of Optics and Fine Mechanics, Chinese Academy of Sciences, Hefei 230031, China*

[b] *Electric Power Research Institute, State Grid Anhui Electric Power Company, Hefei 230031, China*

* *Author to whom correspondence should be addressed. Email: yhfang@aiofm.ac.cn*

Abstract: Photoacoustic (PA) spectroscopy technology has proved to be effective in detection of SF_6 decomposition products. But in the real application environment, the stability of PA spectroscopy device is strongly affected by the ambient temperature. In this paper, we took CO as an example to analyze the impact mechanism of temperatures and the temperature correction formula of response factor of carbon monoxide (PA signal corresponding to unit concentration gas) was derived. The real temperature properties of SF_6 and CO were studied using the non-resonant PA spectroscopy device designed by our team. The study indicates that the PA signals of SF_6 and CO are inversely proportional to temperature, which coincides with the theoretical derivation. A temperature correction method was proposed based on theoretical derivation combined with experimental study and this method was tested and validated. The results show that the relative errors of calculation concentrations of CO acquired by the correction method compared to the actual concentrations are all within 10%, which meet the detection requirements for SF_6 decomposition products of PA spectroscopy in Gas Insulated Switchgear. The correction method has provided an effective way for studying the temperature correction in PA detection for SF_6 decomposition products in GIS.

Keywords: PA Spectroscopy; Temperature correction; Response factor; Background PA signal

1 Introduction

SF_6 enclosed Switchgear has small size and excellent technical performance, which make it an advanced high-voltage electrical distribution equipment in the early 1970s .Such devices are referred to as Gas-Insulator Switchgear, which is abbreviated to GIS, by international community. GIS is a combination of circuit breakers, bus bars, isolating switches, current transformers, voltage transformers and surge arresters casing etc. In GIS, SF_6 is used as the insulated medium. Its insulation properties and arc blow-out performance are both much better than the air.

In Gas Insulated Switchgear(GIS), under the action of Partial Discharge (PD) and superheat, the insulating medium SF_6 will decompose and those decomposition components will react with trace O_2

and H_2O, and further generate SO_2, SOF_2, SO_2F_2, CO and CF_4 etc [1,2]. Preliminary study indicates that under different PD insulating faults, the decomposition products of SF_6 will be different in types, content, production rate and ratio. In the discharge and thermal decomposition process, under the action of moisture, the main decomposition products of SF_6 are SO_2, SOF_2, HF and SO_2F_2. When the faults relate to solid insulating materials, CO, CF_4 and CO_2 are also produced. In that case, we can establish the relationship between SF_6 decomposition and PD types and then determine the cause and the extent of the risk of PD.

Photoacoustic (PA) spectroscopy detection system with high sensitivity and good stability is easy to implement instrumentation and could achieve on-line monitoring, which make it especially suitable for the on-line detection of SF_6 decomposition products in GIS. At present, it has become a hot research field in trace gas detection and has great application prospects. Study shows that the stability and accuracy of PA detection system could be affected by many environmental factors, such as temperature, pressure, humidity and vibration [3-5]. The PA detection device for SF_6 decomposition products in GIS is inevitably affected by these factors, among which ambient temperature is particularly evident. The non-resonant PA cavity designed by our team was fitted with a temperature sensor, which could monitor the real-time changes of temperature inside the cavity, in order that we could study the temperature properties of PA detection for SF_6 decomposition products in GIS. In the detection of SF_6 decomposition products, SF_6 is the carrier gas, which could absorb infrared light and produce background PA signal, and the failure gases such as CO, SO_2 and CF_4 are the components to be analyzed. In this paper, we took CO as an example to analyze the impact mechanism of temperatures. Firstly, the impact mechanism of temperatures was analyzed theoretically and the temperature correction formula of response factor of carbon monoxide (PA signal corresponding to unit concentration gas) was derived. Then, lots of trials were made to study the real temperature properties of pure SF_6 and CO using the non-resonant PA spectroscopy device designed by our team. A temperature correction method was proposed based on theoretical derivation combined with experimental study and the method was tested and validated and the results show that it has provided an effective way for studying the temperature correction method in PA detection for SF_6 decomposition products in GIS.

2 The principles of PA spectroscopy and the detection device

Gas molecules sealed in PA cell are excited to high energy levels after absorbing the modulated irradiation energy, and then de-excited in a non-radiative way and generate heats which could in turn result in periodic pressure fluctuation. With highly sensitive microphones, the pressure fluctuation can be detected and converted into PA electric signal [6-8]. According to the quantitative relationship between the PA signal and the gas concentration, we could get the gas volume fraction by detecting the PA signal.

The PA voltage signal converted from microphone can be expressed as:

$$U = S_{\min} \cdot P_s \cdot C_{cell} \cdot N \cdot \sigma \qquad (1)$$

Where $S_{\min}$ is the microphone sensitivity (mV / Pa), P_s is the source power (W), C_{cell} is the PA cell constant (Pa · cm / W), which generally relates to PA cell size and the physical constants of carrier gas, etc. N is the total number of molecule per unit volume (mol/cm^3), σ is the absorption cross-section of the gas (cm^2/molec).

As is seen in Eq. (1), when the other parameters remain unchanged, there is a good linear relationship between the PA signal and the gas concentration, so by calibrating the relationship equation between the PA signals and the concentrations of the measured gas, the concentrations can be calculated.

Our non-resonant PA detection device is shown in Fig. 1.The non-resonant PA cavity designed by our team was fitted with a temperature sensor, which could monitor the real-time changes of temperature inside the cavity, in order that we could study the temperature properties of PA detection for SF_6 decomposition products. The profile schematic of our non-resonant cell fitted with temperature sensor is shown in Fig. 2. The LM335 temperature sensor operates from -40℃ to 100℃ and the measurement accuracy of it is 1℃.

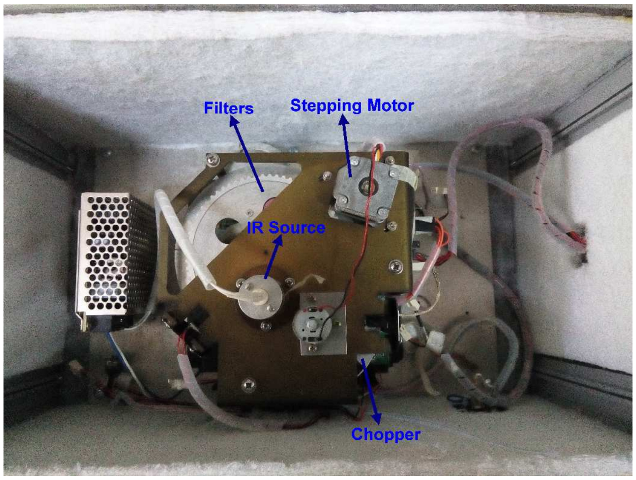

Figure 1 Photo of non-resonant PA detection device

The detector device consists of a light source (IR 19), a chopper (chop frequency, 30Hz), filters, PA cell, a microphone, a control module which controls the rotation of the chopper plate and disc filter, and data acquisition and processing modules. The light passed through the filter after chopping into the PA cell, then a data acquisition module collected PA signal and sent it into the data processing module for processing, and finally through further analysis the type and concentration of the gas were obtained. Schematic diagram of non-resonant PA detection device is shown in Fig. 3. The equivalent radius and length of cylindrical PA cell are 9 mm and 50mm respectively. The microphone that we have used is the G.R.A.S. Microphone Type 40AE and the sensitivity of it is 50 mV/Pa.

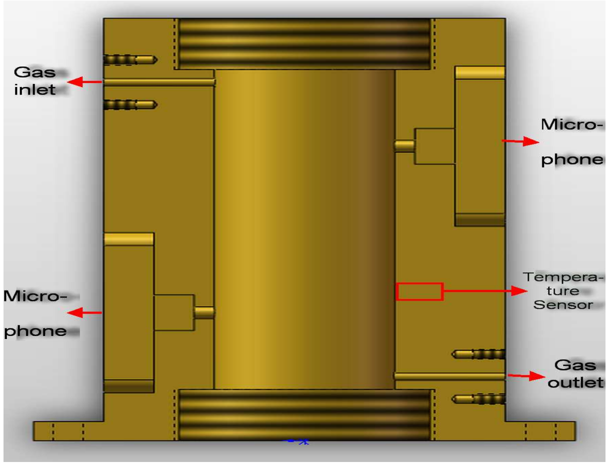

Figure 2 The profile schematic of our non-resonant cell with temperature sensor

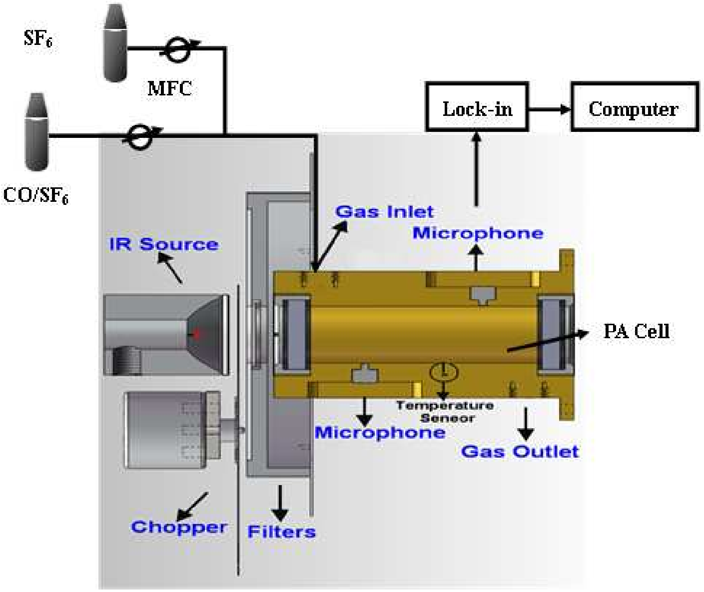

Figure 3 Schematic diagram of non-resonant PA detection device. MFC is the abbreviation of Mass Flow Controller.

3 Theoretical analysis of the temperature's impact on PA signals

The influence of temperatures on PA cell constant and molecular cross-section could reflect how ambient temperatures affect PA signals. In the detection of SF_6 decomposition products, SF_6 is the carrier gas and the failure gases such as CO, SO_2 and CF_4 are the components to be analyzed. In this paper, we took CO as an example to analyze the impact mechanism of temperatures and the temperature correction formula of response factor of carbon monoxide (PA signal corresponding to unit concentration gas) was derived.

3.1 Impact of Temperature on PA Cell constant

For non-resonant cell, the cell constant expression can be expressed as Eq. (2):

$$C_{cell} = \frac{i(\gamma - 1)}{\omega \pi a^2 [1 + (i / \omega \tau_T)]} \qquad (2)$$

Where $\tau_T \approx C_v R^2 / (2.048K)$, $\gamma = C_p / C_v$, C_v, C_p, γ and K are heat capacity at constant volume, heat capacity at constant pressure, adiabatic index and thermal conductivity of carrier gas respectively. The cell constant, which is related to the cell's structure as well as the physical constants of carrier gas and irrelated to target components, could represent the conversion ability of PA cell, which could convert the optical energy into acoustic energy. In the detection of SF_6 decomposition products, SF_6 is the carrier gas. C_v, C_p, γ and K corresponding to SF_6 are all temperature dependent. By referring to Matheson Gas Data Sheet [9], the relationships between these parameters and temperatures can be derived and furthermore the PA cell constants at different temperatures can be obtained. The results are shown in Tab.1 and Fig. 4.

Table 1 The values of C_p, C_v, γ, K and C_{cell} at different temperatures

Temperature(K)	C_p(J/(mol·k))	C_v(J/(mol·K))	γ	K(W/(m·K))	C_{cell}(Pa·cm/W)
273.15	90.635	82.335	1.1008	0.01200	1317.6
278.15	91.729	83.429	1.0995	0.01236	1302.1
283.15	92.823	84.523	1.0982	0.01270	1286.7
288.15	93.917	85.617	1.0969	0.01302	1271.2
293.15	95.011	86.711	1.0957	0.01335	1255.7
298.15	96.105	87.805	1.0945	0.01367	1240.2
303.15	97.199	88.899	1.0934	0.01400	1224.8
308.15	98.293	89.993	1.0922	0.01433	1209.3
313.15	99.387	91.087	1.0911	0.01466	1193.8
318.15	100.481	92.181	1.0900	0.01498	1178.3
323.15	101.575	93.275	1.0890	0.01531	1162.9

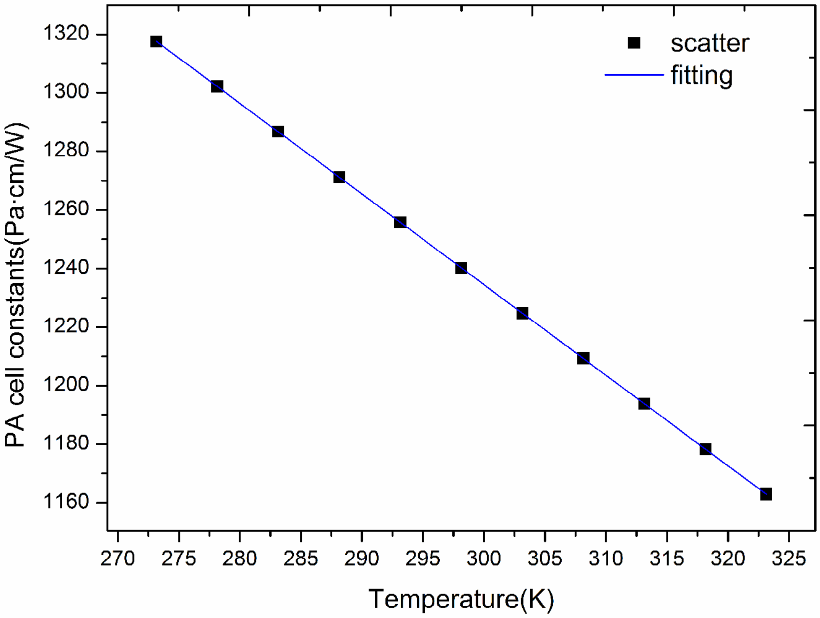

Figure 4 Schematic of variation of PA cell constants with temperature

As can be seen from Fig. 4, the PA cell constant is inversely proportional to temperature and the relational expression of temperature and PA cell constant can be obtained using linear regression fitting method:

$$C_{cell} = -3.095 * T + 2163 \tag{3}$$

Thus the cell constant has negative temperature characteristic, which can be seen from the analysis above.

3.2 Impact of Temperatures on Absorption Cross-section

Absorption cross-section of one single line at any temperature and pressure can be calculated by line integrals. According to the theory of quantum mechanics and spectroscopy, the absorption cross-section can be represented as product of the intensity of the absorption, linear function, and the number of particles per unit volume [10]. The formula is shown in Eq. (4).

$$\sigma(\nu) = S \cdot g(\nu) \cdot N \cdot P \cdot \frac{296}{T} \tag{4}$$

Where σ (ν) is the cross-section of one single absorption line at a wave number of ν, S is the molecular absorption line intensity, N is the number of particles per unit volume and g (ν) is the normalized linear function.

In the non-standard state, the molecular absorption line intensity S can be expressed as Eq. (5).

$$S(P,T)=S(P_0,T_0)\cdot\frac{T_0}{T}\cdot\frac{P}{P_0}\cdot\frac{Q(T_0)}{Q(T)}\cdot\exp\left[-1.439E_1(\frac{T_0-T}{T_0T})\right]\cdot\frac{1-\exp(-hc\nu/kT)}{1-\exp(-hc\nu/kT_0)} \quad (5)$$

Where, *S* (P_0, T_0) is a strong line intensity of standard conditions, *Q* (T_0) is the total partition function under standard conditions, both of which refer to standard HITRAN 2004 database. *P* and *T* are the pressure and temperature of non-standard state.

Since the absorption bands of monocomponent consist of thousands of absorption lines and some of these lines may overlap, the absorption cross-section at the wave number of ν can be expressed as Eq. (6).

$$\sigma_\Sigma(\nu)=\sum_{i=1}^{n}\sigma_i(\nu)=\sum_{i=1}^{n}S(P,T)_i\cdot g_i(\nu)\cdot N\cdot P\cdot\frac{296}{T} \quad (6)$$

As is seen in Eq. (5) and Eq. (6), the single absorption cross-section of the gas is a function of temperature and pressure. Here we just talk about the impact of temperatures on the gas absorptions. In the PA detection of SF_6 decomposition product, the central wavelength of CO was selected at 4.7μm and in that case, the range of 4.56μm~4.84μm wavelength was selected to study the influence of temperatures on absorption cross-section of CO.

The absorption cross-section of single CO molecule at different temperatures of 276K and 316K can be calculated using Line-By-Line method combining the HITRAN2004 database (a pressure of 0.1MPa), as is shown in Fig.5. Similarly, the relationship between total absorption cross-section of CO within the range of 4.56μm ~ 4.84μm wavelength and temperature can be obtained and shown in Fig.6.

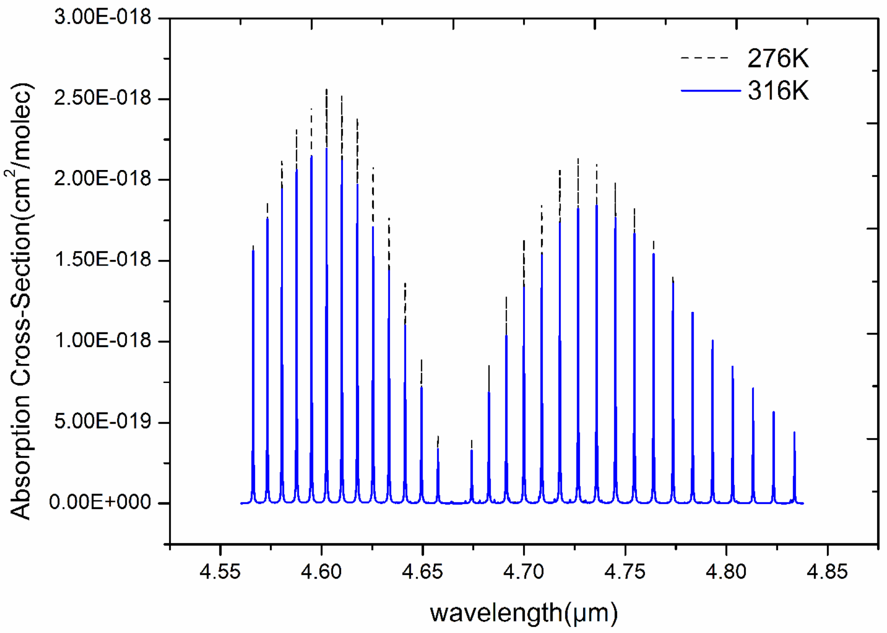

Figure 5 Schematic of absorption cross-sections of single CO molecule at different temperatures

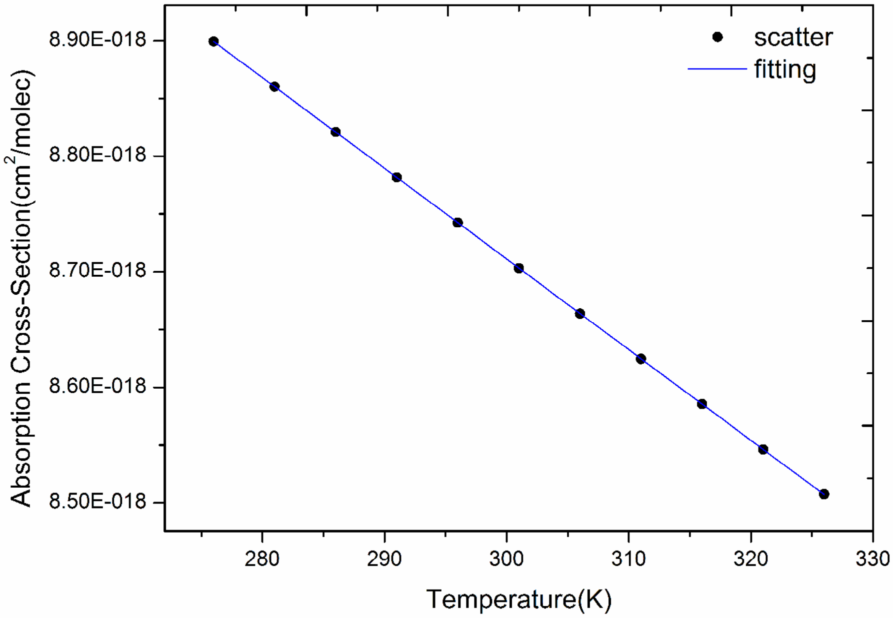

Figure 6 Schematic of variation of total absorption cross-sections of CO (4.56μm~4.84μm) with temperatures

As is shown in Fig.6, the absorption cross-section of CO within the range of 4.56μm ~ 4.84μm wavelength is inversely proportional to temperature and a linear equation can be obtained using a linear regression fitting:

$$\sigma = -7.824 \times 10^{-21} \cdot T + 1.106 \times 10^{-17} \qquad (7)$$

As can be seen from Eq. (1), Eq. (3) and Eq. (7), the PA signal of CO within range of 4.56μm ~ 4.84μm has a negative temperature characteristic.

4 Temperature Correction of PA signal

We have derived the relational expressions of cell constant and absorption cross-section of CO with temperature respectively. Below, a temperature correction method will be proposed based on theoretical derivation combined with experimental study.

4.1 The theory derivation of temperature correction of PA signal

Considering the existence of background absorption [11-16], the concentration inversion formula can be expressed as Eq. (8).

$$U = S_{\min} \cdot P_s \cdot C_{cell} \cdot N \cdot \sigma + b_G \qquad (8)$$

Where b_G is the background PA signal under specific filter.

There is a good linear relationship between PA signals and the concentrations of measured gases, if these parameters, such as: S_{min}, P_s, C_{cell} and σ, are not changed.

$$U = a \cdot N + b \tag{9}$$

Where slope *a*, which is defined as response factor, stands for the PA signal produced by unit measured gas in V/ (μL/L) and intercept *b* is the estimated value of background signal under specific filter b_G in V. Response factor a and background PA signal b can be expressed as Eq. (10) and Eq. (11) respectively:

$$a = S_{\min} \cdot P_s \cdot C_{cell} \cdot \sigma \tag{10}$$

$$b = S_{\min} \cdot P_s \cdot C_{cell} \cdot \sigma_{SF_6} \tag{11}$$

As can be seen from Eq. (9), Eq. (10) and Eq. (11), the temperature correction of PA signal can be converted into the correction of response factor *a* and background PA signal *b*.

Firstly, we will derive the correction formula of response factor, theoretically. If the reference temperature is T_0, the response factor a_0 corresponding to reference temperature could be expressed as Eq. (12).

$$a_0 = S_{\min} \cdot P_s \cdot C_{cell}(T_0) \cdot \sigma(T_0) \tag{12}$$

The response factor a_T corresponding to measured temperature *T* can be expressed as Eq. (13).

$$a_T = S_{\min} \cdot P_s \cdot C_{cell}(T) \cdot \sigma(T) \tag{13}$$

Combining Eq. (3) and Eq. (7), we can obtain Eq. (14):

$$\frac{a_0}{a_T} = \frac{-3.095 \cdot T_0 + 2163}{-3.095 \cdot T + 2163} \cdot \frac{-7.824 \times 10^{-4} \cdot T_0 + 1.106}{-7.824 \times 10^{-4} \cdot T + 1.106} \tag{14}$$

Where T_0 and a_0 are both known and in that case we can calculate the response factor a_T under measured temperature *T* using Eq. (14).

Schematics of relationship between concentrations and PA signals of CO corresponding to three different temperatures are shown in Fig. 7, which are drawn according to the response factors derived from Eq. (14). Here T_0 is 30 and a_0 is 0.001130V/ (μL/L).

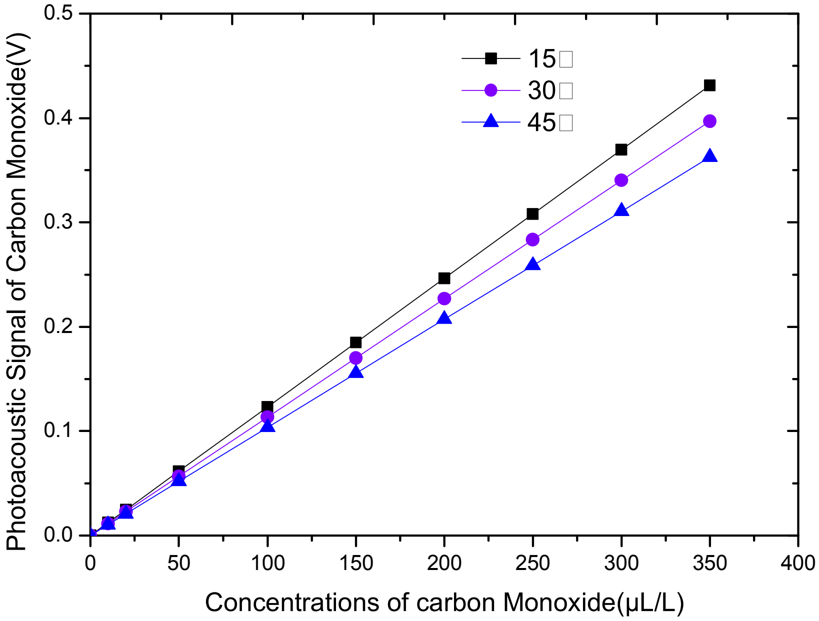

Figure 7 Schematics of relationship between concentrations and PA signals of CO corresponding to three different temperatures

As is shown in Fig. 7, the changes of PA signals caused by unit temperature vary with the concentrations. Although in practical application we cannot correct the PA signal directly without knowing the concentrations of measured gas, we can also correct the response factor according to Eq. (14) to decrease the errors caused by the changes of ambient temperatures.

4.2 Temperature Correction of Background PA signals

As was mentioned above, the temperature correction of PA signals could be converted into the correction of response factors and background PA signals**,** and furthermore the correction formula of response factor has been derived. So a further discussion on the temperature correction of background PA signal is expanded.

In the detection of SF_6 decomposition products, SF_6 is the carrier gas, which has been mentioned before. As is shown in Fig. 8, SF_6 has a plurality of absorption peaks in the requisite infrared wave range and inevitably interferes with other gases. So there will be background absorptions to a certain extent corresponding to different filters. The background PA signal corresponding to specific filter could be considered as a fixed value when the external environment conditions stay permanent [17-21], because SF_6 is the major component of measured gas.

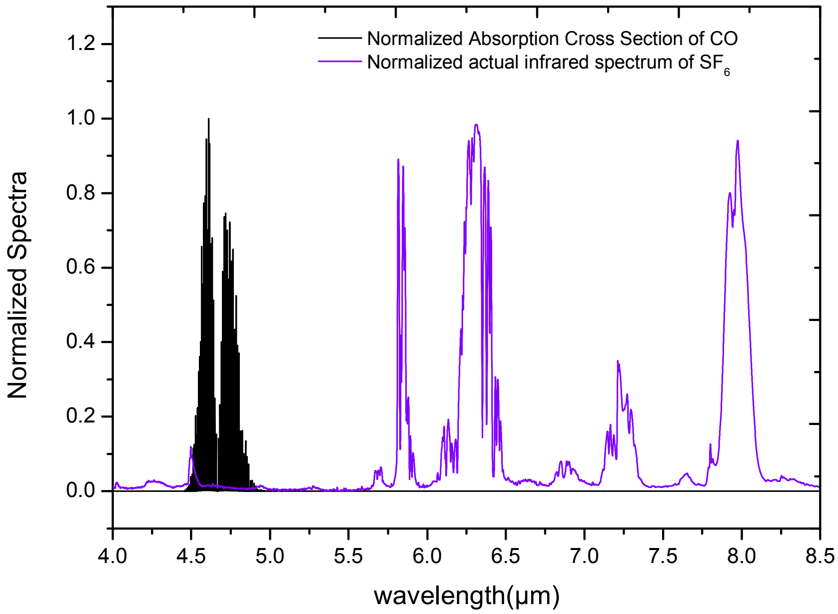

Figure 8 Schematic of measured infrared spectrum of SF_6 and the absorption cross-sections of CO, both of which are normalized

According to the theory of quantum mechanics and spectroscopy, the absorption cross-section of single SF_6 molecule is also the function of temperature and it will vary with the temperatures inside the acoustic cavity, which could result in the changes of background PA signal corresponding to specific filter [22-24]. The accuracy of calculated concentrations could be affected by the variation of background PA signal caused by temperature, so the background PA signal under specific filter also needs to be corrected.

In the PA detection of SF_6 decomposition products, the central wavelength of CO is selected at 4.7μm. But the spectrum lines of SF_6 within 4.7μm wavelength range are not provided in HITRAN database. In that case, the relationship between temperatures and the background PA signals corresponding to CO filter can only be determined through experiments.

4.3 Experimental analysis of Temperature correction of PA signal

In order to study the influence of temperature on the PA detection of SF_6 decomposition products, the non-resonant photoacoustic cavity designed by our team was fitted with a temperature sensor, which could monitor the real-time changes of temperature inside the cavity. As mentioned above, the relationship between temperatures and the background PA signals corresponding to CO filter cannot be derived from theory analysis and can only be determined through experiments [25-27]. The measurement was performed filling pure sulphur hexafluoride (with 99.98% purity) into the PA cell and the inflation process lasted two minutes, and then the experiment began, and then the PA signals and temperature signals corresponding to CO filter were acquired simultaneously. In order to improve the measurement precision, the gross errors of measuring results were removed using Grubbs criterion and the testing values of repeated measurements were averaged. The temperature of PA cell varied due to the continuously heating by the light source. The experiment process (the inflation and measurement process both included) was repeated 5 times and the background PA signals under CO filter corresponding to different temperatures were obtained. The fitting result using quadratic polynomial method is shown in Fig. 9.

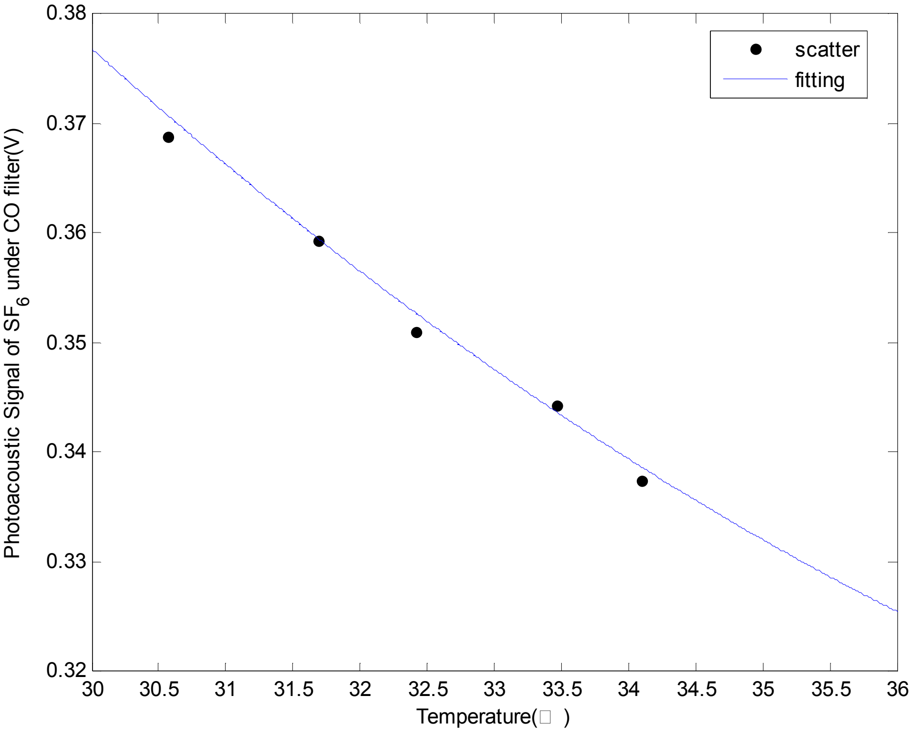

Figure 9 The fitting relationship between temperatures and the background PA signals under CO filter

The background PA signal corresponding to temperature T could be derived from Eq. (15):

$$b_T = b_0 \cdot \frac{y(T)}{y(T_0)} \tag{15}$$

Where the background PA signal b_0 and the reference temperature T_0 are both known and y represents the fitting function of temperatures and background PA signals under CO filter. The background PA signal corresponding to any temperatures could be derived from Eq. (15).

In order to study the temperature properties of CO through experiments, a 100μL/L mixture of carbon monoxide in SF_6 was filled in the PA cell and the air inflation process lasted two minutes. Experimental procedure was the same as above. As was mentioned before, SF_6 had infrared absorption spectrum lines corresponding to CO filter, thus the measured PA signals of 100μL/L carbon monoxide in SF_6 under CO filter comprise the PA signals produced by CO and SF_6. PA signals, which have deducted the background PA signals, are the actual PA signals caused by 100μL/L CO. Keep it in mind that the background PA signals should be corrected according to the corresponding temperatures [28]. The PA signals of 100μL/L CO corresponding to different temperatures, which are obtained according to the procedure above, are shown in Tab. 2.

Table 2 PA signals of 100μL/L CO corresponding to different temperatures

T(□)	28	29	30	31
PA signal(V)	0.1212	0.1191	0.1144	0.1138

As can be seen from Tab. 2, the PA signal of CO has a negative temperature characteristic, which is consistent with the theoretical analysis and also we can learn it from Fig. 7 that the relationship of temperatures and PA signals of carbon monoxide is related to the concentrations of measured carbon monoxide [29]. Thus, when the concentration of measured CO is unknown, we cannot do the temperature correction directly. Fortunately, the response factors can be corrected according to Eq. (14), which would decrease the errors caused by the changes of temperatures.

As was mentioned above, both of the correction formulae of response factor and background PA signal were derived, thus on the basis of corrections of response factor and background PA signal, a temperature correction method was proposed based on theoretical derivation combined with experimental study [30,31]. The specific process is shown in Fig. 10:

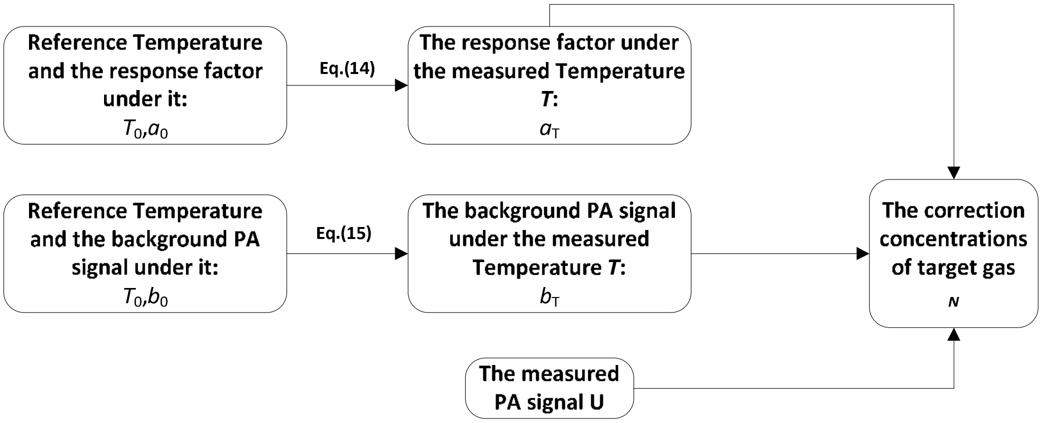

Figure 10 The flow chart of temperature correction of PA signal

The reference temperature T_0 as well as the response factor a_0 and the background PA signal b_0 corresponding to T_0 was stored in the program beforehand. When we calculate the concentrations of carbon monoxide, first of all, the response factor a_T and background PA signal b_T corresponding to measured temperature T should be obtained according to Eq. (14) and Eq. (15) and then the concentrations of CO can be calculated using Eq. (16) below.

$$N = (U - b_T) / a_T \tag{16}$$

Where U is the measured PA signal of carbon monoxide in V, N is the volume concentration in μL/L and a_T and b_T are the response factor and background PA signal corresponding to temperature T.

The contrasts of the calculated and actual concentrations before and after temperature correction procedures are shown in Tab. 3. The result detected by Gas Chromatography was regarded as the actual value of the concentration.

Table 3 The contrast of the calculated and the actual concentrations before and after temperature correction

Actual concentration (μL/L)	Temperature (℃)	Calculation concentration (μL/L)	Relative errors (%)	Correction concentrations (μL/L)	Relative errors (%)
80	32	19.79	75.27	80.72	0.90
80	32	18.79	76.52	79.70	0.37
150	31	141.36	5.76	159.88	6.59
150	31	117.07	21.96	135.08	9.95
300	32	254.63	15.12	321.25	7.08
300	32	242.22	19.26	308.53	2.84
300	32	238.30	20.57	304.52	1.51

Where the result detected by Gas Chromatography was regarded as the actual concentration and the calculation concentration indicated the concentrations before temperature correction. Reference temperature is 30℃

As is shown in Tab. 3, the relative errors of concentrations have mainly decreased after temperature correction and all of the relative errors are all less than 10%. The results indicate that this temperature correction method is effective and it can be generalized to other components to be analyzed in the PA detection of SF_6 decomposition products, such as SO_2 and CF_4.

5 Conclusion

The impact mechanism of temperatures was analyzed and the temperature correction formula of response factor of carbon monoxide was derived. The real temperature properties of SF_6 and CO were studied using the non-resonant photoacoustic spectroscopy device filled with temperature sensor designed by our team. The study shows that the PA signals of SF_6 and CO are inversely proportional to temperature, which coincides with the theoretical derivation. A temperature correction method was proposed based on theoretical derivation combined with experimental study and it was tested and validated. The results show that the relative errors of concentrations of CO acquired by the correction method compared to the actual concentration are all less than 10%, which have met the detection requirements for SF_6 decomposition products of PA spectroscopy in GIS. This temperature correction method may provide an effective way for studying the temperature properties in the PA detection of SF_6 decomposition products in GIS.

As were mentioned above, the temperature corrections of the PA signal are on the basis of two aspects: one is the corrections of response factor and the other is the corrections of the background PA signal. In the next step, we will install a temperature control device to keep the temperature of the PA cavity invariant and make further efforts to verify the relationship between response factors and temperatures.

Acknowledgements

This work was supported by Electric Power Research Institute of Anhui Province who provided

the essential experimental materials, such as the calibrating gases and the electric mass-flow controller.

References

1. Y. W. Liu, L. Y. Wu and Y. P. Gong, *Power System Technology*, 2009, 33, 58-61..
2. B. Qi, C. R. Li, L. S. Luo, Y. Zhang and S. S. Zheng, *High Voltage Engineering*, 2010, 36, 957-963.
3. Y. G. Hu, X. X. Zhang, Z. Wang and Z. Y. Zhao, *High Voltage Engineering*, 2011, 37, 1166-1171.
4. W. G. Chen, B. J. Liu, J. X. Hu, H. Y. Zhou and J. Li, *Journal of Chongqing University*, 2011, 34, 7-13.
5. G. Meng, Southwest University of Science and Technology, 2012.
6. S. W. Sun, H. M. Yi, G. S. Wang, L. Wang, T. Tan, K. Liu and X. M. Gao, *CHINESE JOURNAL OF LASERS*, 2012, 39, 209-214.
7. G. Meng, X. Y. Liu, C. Y. Yuan, F. Guo, C. K. Zheng and C. Peng, *Spectroscopy and Spectral Analysis*, 2011, 31, 1819-1822.
8. W. G. Ma, W. B. Yin, T. Huang, Y. T. Zhao, C. Y. Li and T. S. Jia, *Spectroscopy and Spectral Analysis*, 2004, 24, 135-137.
9. C. L. Yaws and S. D. Kad, USA, 7th edn., 2001, ch. 138, pp. 758-762.
10. D. P. Kratz, M. G. Mlynczak, C. J. Mertens, H. Brindley, L. L. Gordley, J. Martin-Torres, F. M. Miskolczi and D. D. Turner, *Journal of Quantitative Spectroscopy & Radiative Transfer*, 2005, 90, 323-341.
11. M. S. Niu, Q. Liu, K. Liu, Y. Q. Yuan and X. M. Gao, *Optics Communications*, 2013, 287, 180-186.
12. R. A. Rooth, A. J. L. Verhage and L. W. Wouters, *APPLIED OPTICS*, 1990, 29, 3643-3653.
13. M. Szakáll, J. Csikós, Z. Bozóki and G. Szabó, *Infrared Physics &Technology*, 2007, 51, 113-121.
14. J. V. Beitz, B. M. Hinaus and J. Huang, *APPLIED OPTICS*, 1994, 33, 921-929.
15. A. Schmohl, A. Miklós and P. Hess, *APPLIED OPTICS*, 2002, 41, 1815-1823.
16. A. Miklos, C-H. Lim, W-W, Hsiang, G-C, Liang, A. H. Kung, A. Schmohl and P. Hess, *APPLIED OPTICS*, 2002, 41, 2985-2993.
17. M. A. Gondal, A. A. I. Khalil and N. Al-Suliman, *APPLIED OPTICS*, 2012, 51, 5724-5734.
18. A. Glière, J. Rouxel, M. Brun, B. Parvitte, V. Zéninari and S. Nicoletti, *Sensors*, 2014, 14, 957-974.
19. P. Patimisco, G. Scamarcio, F. K. Tittel and V. Spagnolo, *Sensors*, 2014, 14, 6165-6206.
20. C. B. Hirschmann, N. S. Koivikko, J. Raittila, J. Tenhunen, S. Ojala, K. Rahkamaa-Tolonen, R. Marbach, S. Hirschmann and R. L. Keiski, *Sensors*, 2011, 11, 5270-5289.
21. M. Rocha, M. Sthel, G. Lima, M. da. Silva, D. Schramm, A. Miklós and H. Vargas, *Sensors*, 2010, 10, 9359-9368.
22. A. Pohlkötter, M. Köhring, U. willer and W. Schade, *Sensors*, 2010, 10, 8466-8477.
23. B. Ageev, Y. Ponomarev and V. Sapozhnikova, *Sensors*, 10, 3305-3313.
24. M. A. Gondal, A. Dastageer and M. H. Shwehdi, *Talanta*, 2004, 62, 131-141.
25. V. Hanyecz, A. Mohácsi, A. Pogány, A. Varga, Z. Bozóki, I. Kovács and G. Szabó, *Vibrational Spectroscopy*, 2010, 52, 63-68.
26. A. Beenen and R. Niessner, *Analyst*, 1998, 123, 543-545.
27. S. Schilt, L. Thévenaz, M. Niklès, Lukas Emmenegger and C. Hüglin, *Spectrochimica Acta Part A*, 2004, 60, 3259-3268.
28. V. Koskinen, J. Fonsen, K. Roth and J. Kauppinen, *Vibrational Spectroscopy*, 2008, 48, 16-21.
29. A. A. Kosterev, Y. A. Bakhirkin and F. K. Tittel, *Appl. Phys. B*, 2005, 80, 133-138.
30. J. Uotila, *Infrared Physics & Technology*, 2007, 51, 122-130.

31. J. D. Nikolić, M. D. Rabasović, D. D. Markushev and J. Jovanović-Kurepa, *Optical Materials*, 2008, 30, 1193-1196.

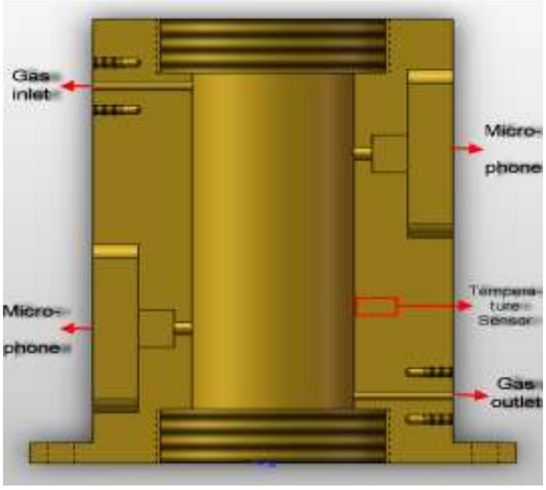

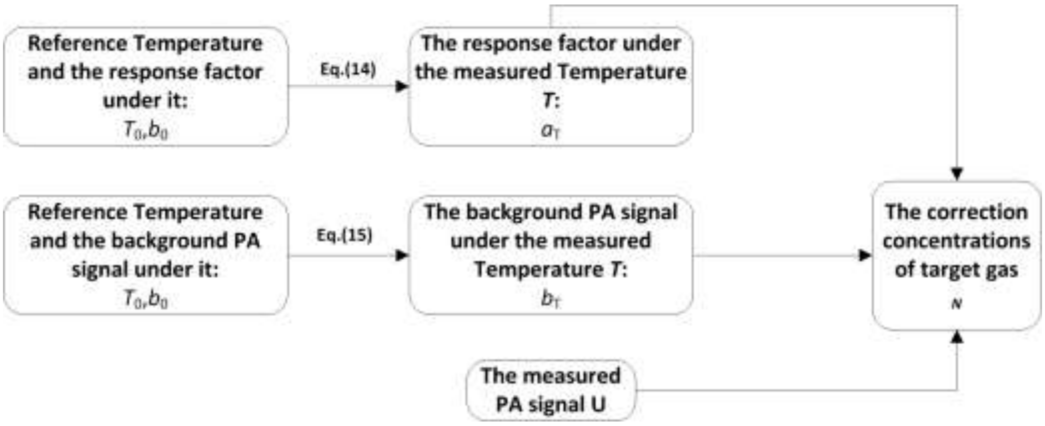

$$\frac{a_0}{a_T}=\frac{-3.095\cdot T_0+2163}{-3.095\cdot T+2163}\cdot\frac{-7.824\times10^{-21}\cdot T_0+1.106\times10^{-17}}{-7.824\times10^{-21}\cdot T+1.106\times10^{-17}} \tag{14}$$

$$b_T=b_0\cdot\frac{y(T)}{y(T_0)} \tag{15}$$

Photoacoustic (PA) spectroscopy technology has proved to be effective in detection of SF_6 decomposition products. But in the real application environment, the stability of PA spectroscopy device is strongly affected by the ambient temperature. In this paper, we took CO as an example to analyze the impact mechanism of temperature and the temperature correction formula of response factor of carbon monoxide (PA signal corresponding to unit concentration gas) was derived. The real temperature properties of SF_6 and CO were studied using the non-resonant PA spectroscopy device designed by our team. The study indicates that the PA signals of SF_6 and CO are inversely proportional to temperature, which coincides with the theoretical derivation. A temperature correction method was proposed based on theoretical derivation combined with experimental study and this method was tested and validated. The results show that the relative errors of calculation concentrations of CO acquired by the correction method compared to the actual concentrations are all within 10%, which meet the detection requirements for SF_6 decomposition products of PA spectroscopy in Gas Insulated Switchgear. The correction method has provided an effective way for studying the temperature correction in PA detection for SF_6 decomposition products in GIS.